Article

Groundwater Bioremediation through Reductive Dechlorination in a Permeable Bioelectrochemical Reactor

Geremia Sassetto [ID], Laura Lorini [ID], Agnese Lai, Marco Petrangeli Papini [ID] and Marco Zeppilli *[ID]

Department of Chemistry, University of Rome Sapienza, P.le Aldo Moro 5, 00185 Rome, Italy;
geremia.sassetto@uniroma1.it (G.S.); laura.lorini@uniroma1.it (L.L.); marco.petrangelipapini@uniroma1.it (M.P.P.)
* Correspondence: marco.zeppilli@uniroma1.it

Abstract: A new membrane-less bioelectrochemical reactor configuration was developed for contaminated groundwater remediation. The new bioelectrochemical reactor configuration was inspired by the utilisation of a permeable reactive barrier (PBR) configuration with no separation membrane. The corresponding reactive zones were created by using graphite granules and mixed metal oxide (MMO) electrodes to stimulate the reductive and oxidative biological degradation of chlorinated aliphatic hydrocarbons. In the present study, the PBR-like bioelectrochemical reactor has been preliminarily operated with synthetic contaminated groundwater, testing the reductive dechlorination activity on cis-dichloroethylene (cisDCE). Moreover, to assess the effects of competing anions presence for the electron donor (i.e., the cathode), the synthetic wastewater contained sulphate and nitrate anions. In the PBR-like reactor operation, nearly all cisDCE was removed in the initial sampling port, with only VC detected as the observable RD product. During the same biotic test of the PRB reactor, the presence of both the reductive dechlorination and anions reduction was confirmed by the complete nitrate reduction in the cathodic chamber of the PRB reactor. On the contrary, sulphate reduction showed a lower activity; indeed, only 25% of the influent sulphate was removed by the PRB reactor.

Keywords: reductive dechlorination; oxidative dechlorination; bioremediation; microbial electrolysis cells

1. Introduction

Chlorinated aliphatic hydrocarbons (CAHs) like tetrachloroethane (1,1,2,2 TeCA) and TCE are problematic subsurface contaminants due to their widespread industrial use, environmental persistence, and toxicity. Nowadays, perchloroethylene (PCE), TCE, and their degradation intermediates cisDCE and VC are frequently identified groundwater pollutants [1,2]. However, physico-chemical methods to clean up subterranean environments contaminated by CAHs can be prohibitively expensive, particularly for secondary source zone treatment. Therefore, anaerobic bioremediation utilising reductive dechlorination (RD) is considered a cost-efficient and effective remediation technology for CAHs in groundwater. The technology involves utilising anaerobic dechlorinating bacteria to eliminate chlorinated contaminants by incorporating them as terminal electron acceptors in their energy metabolism [3,4]. In anaerobic conditions, several microorganisms can convert highly chlorinated parent CAHs into less-chlorinated daughter CAHs via RD [5,6]. While several dechlorinating organisms like *Dehalobacter* can reduce PCE and TCE to cisDCE, only *Dehalococcoides Mccartyi* spp. can perform RD beyond cisDCE to produce harmless, non-chlorinated ethene [7,8]. Hydrogen gas is identified as a primary electron donor for most dechlorinating bacteria, including *Dehalococcoides* spp. Recently, bioelectrochemical systems that utilise water electrolysis [9] were proposed to provide H₂ to dechlorinating bacteria. To enhance in situ bioremediation technologies, bioelectrochemical systems (BES) have been proposed to supply electrons required for the RD, a process known as Bioelectrochemically Assisted Reductive Dechlorination (BEARD). Bioelectrochemical systems are advanced

processes that utilise the interaction between polarised electrodes and electroactive microorganisms to address a variety of environmental issues. Examples include hydrogen and methane production from wastewater treatment [10,11], nutrient recovery [12], and pollutant removal [13,14]. These studies have demonstrated that regulating the RD at the electrode surface can be achieved by selecting the appropriate potential [15–17], whether through the use of external redox mediators or nanoparticles or without any additional chemicals altogether [18,19]. The delivery of electrons can be continuously monitored and controlled in terms of current and potential, eliminating the need for chemical injection and subsequent transport, storage, dosing, and post-treatment [20]. CisDCE and VC, in contrast to their heavily chlorinated precursors, exhibit greater susceptibility to biodegradation via oxidative pathways either co-metabolically or metabolically. This process, facilitated by aerobic bacteria thriving on hydrocarbons like methane or ethene, involves the utilisation of dioxygenase or monooxygenase enzymes to transform them into epoxides [21–24]. During the formation process, chlorinated epoxides tend to become unstable and break down into carbon monoxide, formate, glyoxylate, and chlorinated acids [25]. However, when it comes to metabolic degradation, microorganisms usually use CAHs as the only source of carbon and energy for growth and maintenance. Currently, there are four main categories of bioelectrochemical systems utilised for reducing oxidised contaminants, including CAHs. These categories are based on different mechanisms responsible for transferring electrons to microorganisms, the four mechanisms can be described as the hydrogen-mediated mechanisms, the direct electron transfer from the cathodic electrodic surface to the microorganisms, and the presence of endogenous or exogenous redox mediator [26–30]. Through bioelectrochemical systems, electrons are directly and selectively supplied to dechlorinating bacteria growing on the electrode surface rather than using chemicals [28]. This method represents a clean approach to stimulate and control microbial reductive dechlorination reactions. In these bioelectrochemical methods, the rate of hydrogen (and oxygen) supply can be easily controlled by adjusting the electric current, which is a significant advantage. Despite this, it should be noted that none of the above methods allow for direct control over the rate and extent of microbial dechlorination, nor the competition for produced hydrogen between dechlorination and competing metabolisms. However, studies have shown that electrical stimulation of anodic oxidative dechlorination (OD) can occur only when oxygen is electrochemically generated at the electrode surface [29]. The potential obtained at the counter-electrode would enable the development of oxygen, which plays a crucial role in stimulating the microbial cometabolic oxidation of less-chlorinated ethene (cisDCE). The configuration of OD operated downstream of the RD has shown promise in treating groundwater contaminated with CAHs [21]. By implementing this sequential approach, the accumulation of cisDCE and VC in the field could be effectively reduced. As a result, researchers have explored the development of new bioelectrochemical systems that facilitate direct or indirect extracellular electron transfer to dechlorinating bacteria. The RD at the biocathode of the BES reactor has been thoroughly studied under various operational conditions, with the process's performance evaluated using the mass balance of relevant compounds [30,31]. In recent years, there has been extensive investigation into the use of an innovative microbial electrolysis cell (MEC) configuration without a membrane. This setup aims to achieve complete mineralisation of chlorinated aliphatic hydrocarbons in groundwaters through reductive/oxidative treatment [32]. A new and innovative approach has been developed for creating bioelectrochemical reactors that are both scalable and effective. This configuration uses an internal graphite counter electrode as a sacrificial material to stimulate reductive and oxidative dechlorination. To test the process, a laboratory-scale bioelectrochemical system was created, consisting of a reductive and an oxidative MEC. The system was tested with different contaminated feeding solutions, including an optimised mineral medium (MM), synthetic groundwater (SG), and real contaminated groundwater (Rho GW). Various hydraulic retention times (HRTs) and electrodic potentials were also tested. The results showed that highly chlorinated compounds like PCE and TCE were effectively removed by the reductive reactor in all the explored conditions (i.e., MM, SG,

and Rho GW), being mostly reduced into cis DCE and/or VC depending on the operating conditions (i.e., HRT and electrodic potential) [33,34]. However, the presence of sulphate and nitrate in the synthetic groundwater solution caused sulphate and nitrate reduction in the reductive reactor, which affected current generation and energy consumption [35]. Additionally, in the oxidative reactor, both oxidative and reductive dechlorination pathways were observed due to the presence of the internal counter-electrode, which acted as an electron donor. Using this sequential reductive/oxidative bioelectrochemical process, complete mineralisation of CAHs in real groundwater was achieved with no significant interference from Fe^{+3} or sulphate [36]. Another lab-scale reactor was designed to investigate the potential for in situ microbial RD using a different reactor configuration. This new PBR-like column had no separation membrane between the sequential cathodic and anodic compartments, and the anode was made of a plastic cylinder mesh (1.2×1.2 mm pore size) with closed ends to maximise the interface area and limit resistance. The cathode was fed in up-flow mode, while the anode acted as a sacrificial anode, minimising water electrolysis and scavenging O_2. The study aimed to evaluate the impact of competitive metabolic processes, such as nitrate reduction and sulphate reduction, on RD. The investigation focused on the presence of anions like sulphate and nitrate and the absence of autochthone microorganisms, which could activate competing mechanisms and affect the efficiency of RD in the system. The novelty of this work lies in testing a new configuration of the system that is simpler and easier to implement. Indeed, compared to previous experimental setups, this configuration alters the spatial arrangement of the electrodes by placing them in two portions of the column and separating them only with an inert silica layer.

2. Results and Discussion

2.1. Groundwater Sampling and Characterisation

The groundwater was sampled from an industrial area located in the north of Italy. To set up the synthetic groundwater, a sample of shallow (5–10 m bgs) groundwater was monitored to have a preliminary characterisation (Table 1). The concentration of chlorinated compounds was detected with gas-chromatography analysis. The results showed a high concentration of the different chlorinated species, PCE, TCE, cisDCE, and VC, with a strong predominance of cisDCE. Usually, cisDCE is not a native contaminant while it is considered the main intermediate of reductive dechlorination [37].

Table 1. CAHs and anions concentrations in the analysed groundwater compared to the concentration limits according to Italian law (CSC, D.lgs 152/06).

	µmol/L	µg/L	(CSC) µg/L
VC	0.34 ± 0.10	21.1	0.5
cisDCE	0.98 ± 0.12	61.1	60
TCE	0.59 ± 0.3	77.3	1.5
PCE	0.09 ± 0.01	15.2	1.1
Chloride	800 ± 16	2910 ± 31	
Nitrate	400 ± 21	2630 ± 40	
Sulphate	2013 ± 40	1895 ± 210	2500

This suggests that an indigenous dechlorinating activity is naturally occurring at the site. Following this evaluation, it was decided to focus on the enhancement of reductive dechlorination of cisDCE. As reported in Table 1, a considerably higher concentration of sulphate and nitrate was detected, indicating possible competition for the available reducing power between the biological sulphate/nitrate reduction reaction and biological reductive dechlorination reaction. Another parameter measured was the conductivity of the groundwater (indicator for total content of dissolved salts), which was high, about the same order of magnitude as the conductivity of the synthetic medium (2.15 mS/cm). The determination of TOC in groundwater samples showed a negligible value since comparable values of the total and inorganic carbon were obtained (around 50 mgC/L).

2.2. Fluid Dynamic Characterisation and Preliminary Abiotic Tests

A conservative tracer experiment has been conducted using sodium bromide in the feeding solution, which was fed at a 5.8 L/d flow rate from the top of the column to port D (cathodic outlet), applying a fixed current of 100 mA, to characterise the fluid dynamic behaviour of the liquid phase and calculating the effective porosity of the packing bed. The F test curve reported in Figure 1 allowed us to determine the effective hydraulic residence time (τ) that resulted in 6.97 h, giving an effective volume of 1.7 L. A porosity of 0.47 was calculated by using the geometric volume of 3.65 L of the reactor hosting the cathodic compartment (i.e., from the top of the column to port D of the reactor). This value was consistent with previous analysis of graphite granules used as reactor filling. Moreover, the shape of the F curve depends on dispersion and the boundary conditions for the vessel. The resulting S-shaped response curves are not symmetrical (Figure 1); this indicates a large deviation from the plug flow (PF) model.
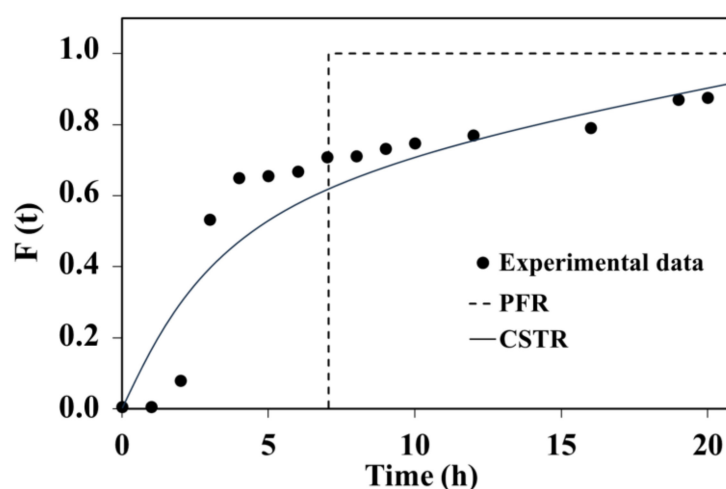

Figure 1. Tracer step experiment for residence time distribution curve F(t) and the theoretical perfect mixing flow (CSTR) and plug flow (PFR) RTD curves in cathodic compartment output (sampling port D).

The PBR reactor was operated in galvanostatic mode at 100 mA for 8 h per day, and it was fed with only mineral medium to preliminarily verify the possibility of creating the anaerobic and reductive conditions for the following inoculum.

During each daily galvanostatic polarisation, the potential difference remained constant around the value of 10 V, while the value of the cathode decreased over time due to the gradual polarisation (Figure 2). After several daily cycles, the cathodic potential became more negative (-640 ± 11 mV vs. SHE). After 30 days of galvanostatic cycles, the cathode potential resulted enough negative, and it became a good environment for reductive dechlorination; on the other hand, the cell voltage between the anode and cathode decreased until -13 V, while the potential of the anode compartment became more oxidising (930 mV vs. SHE). To better understand the production of hydrogen in the system, during the daily 8 h galvanostatic test, H_2 concentration and pH in the three zones (i.e., cathodic, non-conductive and anodic), the potential difference and the anodic potential were observed. As an example, Figure 3 shows a typical trend of H_2 concentration, which also confirms a high concentration of H_2 in the non-conductive zone and a very low level in the cathodic compartment. It shows that the H_2 production took place close to the non-conductive area, and the produced H_2 raised upstream in the cathodic area (Figure 3B), while it was not detected in the anode. This result is also confirmed by the value of pH (Figure 3A) since the production of H_2 involves an increase in pH after the cathodic reaction: ($4H_2O + 4e^- \rightarrow 2H_2 + 4OH^-$). The pH value was constant near the neutrality during the test both in the cathode and the anode, while it became 9 in the

non-conductive area (Figure 3A). A pH increase affected water electrolysis for H_2 formation [38]. Furthermore, the anodic reaction of oxygen led to the hydroxyl ion consumption $(4OH^- \rightarrow O_2 + 2\,H_2O + 4e^-)$.
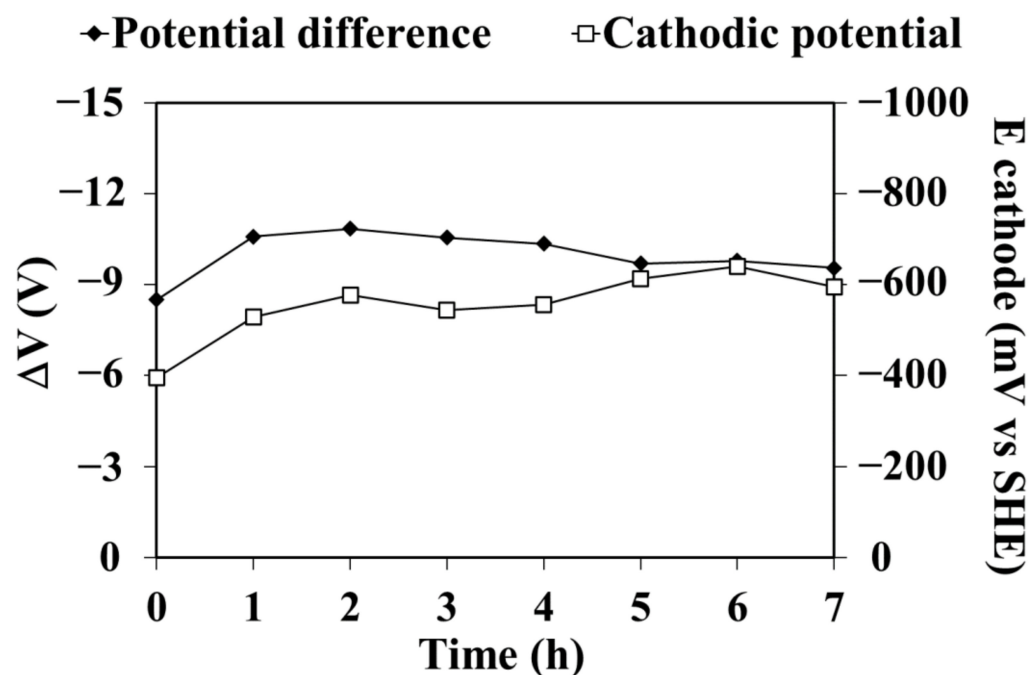

Figure 2. Potential difference and cathodic potential in bioelectrochemical membrane-less PBR-like reactor during a cycle in galvanostatic mode.
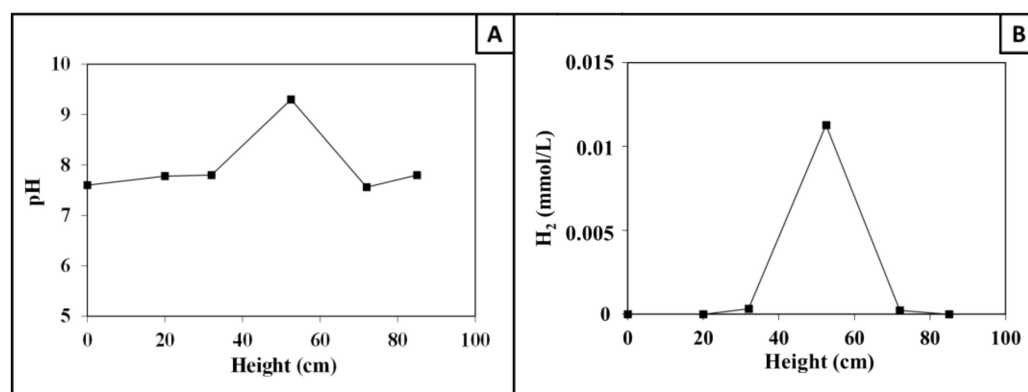

Figure 3. pH (**A**) and H_2 concentration (**B**) in the PBR reactor during the 8 h galvanostatic polarization at 100 mA.

2.3. Synthetic Groundwater Laboratory Test

To start up the reactor, the cathode (between port A and port D) was inoculated with 0.5 L of a TCE-to-ethene dechlorinating culture and 0.2 L of a cisDCE-to-ethene dechlorinating culture, previously enriched on hydrogen and TCE or cisDCE as electron donor and acceptor, respectively. Raw data of the 16S rRNA gene amplicon sequencing of the consortium are available at the DDBJ/ENA/GenBank under the BioProject PRJNA705054 (SRA: SRX10172732). No inoculum was given to the anodic chamber. The bioelectrochemical membrane-less PBR-like reactor was operated in continuous galvanostatic mode by imposing the passage of 100 mA for more than 30 days. Throughout the entire operational period, the cathode chamber of the bioelectrochemical reactor was continuously fed at a flow rate of 5.8 L/d, with an anaerobic medium contaminated with cisDCE to a

final concentration of 24.6 ± 2.8 µmol/L. As previously described, the synthetic medium, which simulated the groundwater composition, was also rich in inorganic anions, such as nitrate and sulphate (Table 1). After a very short lag time where cisDCE was mostly removed by adsorption onto graphite granules, the reductive dechlorination started with the production of cisDCE and VC that were observed at the first sampling port (7 cm of graphite bed). A typical concentration profile of chlorinated compounds is shown in Figure 4. The removal of cisDCE was almost quantitative in the first sampling port, and the only detectable RD product was VC (Figure 4A). The VC formation was a reductive dechlorinating microbial activity indication. However, the overall concentration of all chlorinated compounds decreased along the column to 6.8 ± 0.3 µmol/L, maybe due to their adsorption or some counter-current mass transfer up to the top of the column. Methane production was also evident with the higher concentration observed in the proximity of the cathodic electrode (Figure 4A). Nitrate anions were completely removed in the upper part of the column. The sulphate reduction showed a slower rate since a small variation resulted between the influent and the effluent sulphate concentration (25%) (Figure 4B). Moreover, a back-oxidation in the anodic compartment was observed for about 20% of the reduced sulphate. H_2 and pH profiles confirmed the results shown with the preliminary abiotic tests (Figure 4C,D). The H_2 profile in Figure 4C confirms that the H_2 was produced in the proximity of the non-conductive slice, where its maximum concentration was observed (0.7 ± 0.2 m µmol/L). The H_2 moved the counter-current across the cathode compartment, where it was consumed due to reductive dechlorination and methanogenesis. The pH increased in the cathodic area and reached a maximum in the non-conductive one (Figure 4D). The high value of pH in the non-conductive zone could hinder most biological reactions in both cathodic and anodic sections that were closest in the area.
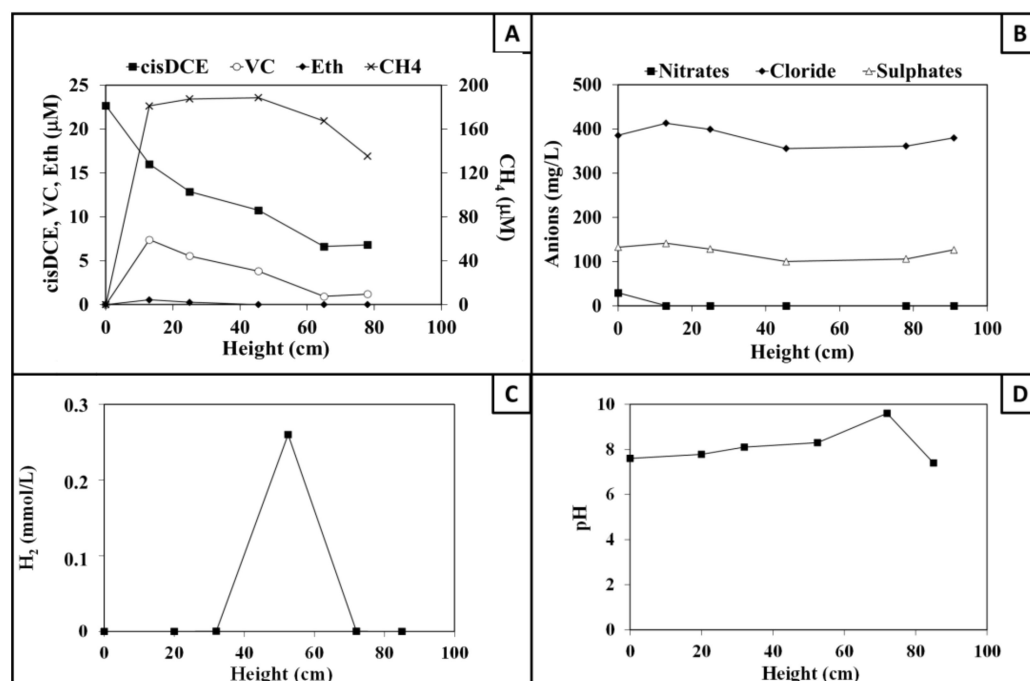

Figure 4. Concentration profile of cisDCE, reduced products and methane (**A**), anions (**B**), hydrogen (**C**) and pH (**D**) along the bioelectrochemical membrane-less PBR-like reactor operating in continuous flow and galvanostatic mode.

After a month of continuous flow operation, the pilot scale PBR-like column reactor had not achieved the steady-state condition yet. The potential difference between the cathode and the anode was rather steady after a few days of polarization, with an average value of −11.1 ± 0.3 V. Moreover, the overall potential difference in the system was quite

higher than the actual difference between the two electrodes and most of the potential drop was concentrated across the non-conductive slice.

Besides instantaneous profiles along the columns, we chose to monitor the system performance over time by using three points only, i.e., the cathode compartment through port B, the cathodic effluent (non-conductive area) through the sampling port D and the anode compartment through the sampling port F. The following graphs (Figure 5C,D) show the concentrations of cisDCE, VC, methane, nitrate and sulphate in the considered sampling ports. From Figure 5A,C, it is evident that most of the influent cisDCE was removed while crossing the cathode compartment with VC as the main product (6.8 ± 0.3 µmol/L).
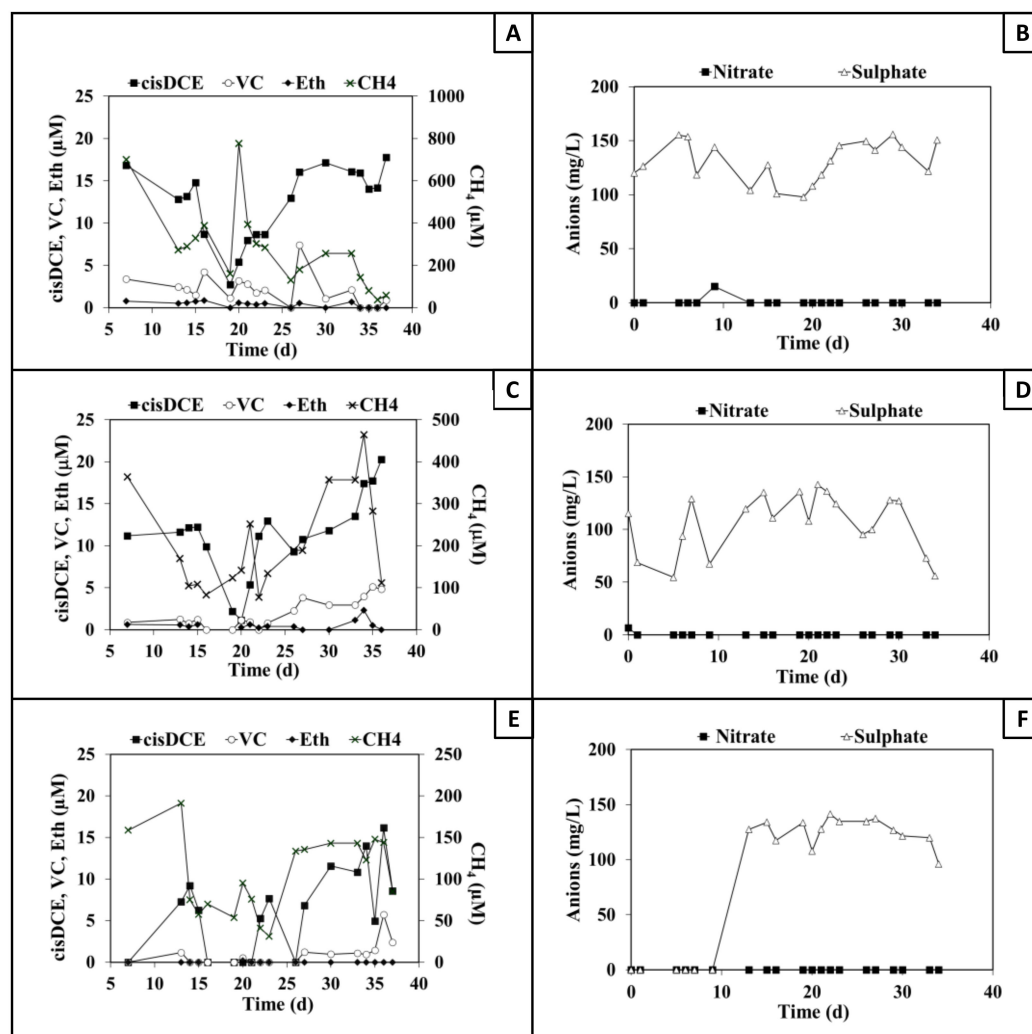

Figure 5. CAHs, ETH, methane (panel **A,C,E**) and anions (panel **B,D,F**) concentration in the sampling port B (cathodic electrode) (panel **A,B**), D (non-conductive area) (panel **C,D**) and F (anode electrode) (panel **E,F**) in the PBR reactor.

During the first 20 working days, the reactor performance increased; in detail, the cisDCE was removed for more than 96%. After approximately 20 days of operation, RD, methane production and anion reduction decreased. The lack of methanogenesis and nitrate reduction was not due to the absence of hydrogen, which was detected all the time (Figure 6), and the hydrogen concentration transient increase confirmed the partially arrested metabolisms.
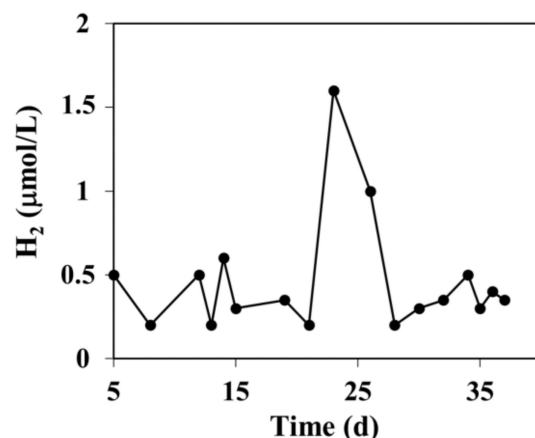
Figure 6. Hydrogen temporal concentration profile in the bioelectrochemical membranelles PBR-like reactor operating in continuous flow in galvanostatic mode.

The only active metabolism was the nitrate reduction, which was complete after a few working days from the reactor start-up. Additionally, the average sulphate concentration in the cathodic effluent was slightly above that of the influent, indicating that sulphate reduction was not active (Figure 5B). However, after a few working days, the RD, sulphate reduction and methanogenesis partially recovered. In particular, cisDCE had a slow reduction, but VC concentration increased from 0.9 ± 0.2 to 3.7 ± 0.4 µmol/L in sampling port D (Figure 5D). For the entire test, a high concentration of methane was detected (Figure 5A,C,D); notably, the concentration at the end of the cathodic zone was double respect to the anodic one, suggesting that methane was oxidised, and it could also be transported by the bulk flow. Time profiles at ports D (nonconductive area) and F (anode compartment) show that both RD intermediates and methane were at a lower level. However, the mechanism of this apparent removal was still unclear. In all investigated conditions, nitrate reduction was complete, and no nitrate was observed at any sampling port for the entire test duration (Figure 5B). Sulphate reduction was also observed, even though a sharp increase was observed after 25 days of operation (Figure 5D). Sulphate concentration in the effluent from the cathodic zone (port D) was almost major to the sulphate concentration leaving the anodic zone (port F); it seemed that sulphate was formed back (i.e., by anodic oxidation). However, a longer operational period would be necessary to confirm this preliminary evidence. The coulombic efficiency was calculated to determine which fraction of the current was used by the different final electron acceptors in sampling port D, that is, the cathodic effluent. Most of the current was consumed by nitrate and sulphate reduction (the latter contribution increased throughout the test), 17.1 and 22.6%, respectively. The methanogenesis contribution (12.4%) was also relevant, whereas the reductive dechlorination accounted for less than 0.1% of the transferred charge. By accounting for all the considered mechanisms (i.e., RD, nitrate reduction, sulphate reduction, methanogenesis and hydrogen formation), the overall coulombic efficiency was about 57% (Figure 7).

In agreement with these results, the energy balance of the system was not complete because only a minor fraction of the current was used in the considered mechanisms, as already described in other literature studies [34,35].

The data obtained in this experimental study have been compared with the performances obtained (under similar HRT conditions) with the internal counter-electrode configuration explored in previous work [35]. As reported in Table 2, the two reactor configurations have been tested under similar conditions of HRT and synthetic groundwater composition (i.e., CAHs in the presence of nitrate and sulphate). The data comparison clearly showed a lower performance of the PRB configuration compared with the internal counter-electrode reactor, which was able to dechlorinate and reduce anions with lower energy consumption, i.e., 0.6 ± 0.1 vs 4.6 ± 0.9 kWh/m^3. Despite the lower per-

formance in terms of dechlorination rate, it is interesting to observe a similar coulombic efficiency for the nitrate reduction while, due to the different sulphate concentrations in the synthetic groundwater, sulphate reduction coulombic efficiency resulted higher in the counter-electrode configuration. The lower performance of the PRB configuration with respect to the internal counter-electrode configuration was mainly caused by the considerable increase in resistance promoted by the setup of the nonconductive layer to separate anodic and cathodic compartments. Indeed, in the counter-electrode configuration, the electrode distance between the anode and cathode is considerably lower at the same time; internal counter-electrode configuration requires more constructive requirements in terms of reactor configuration and materials utilisation.
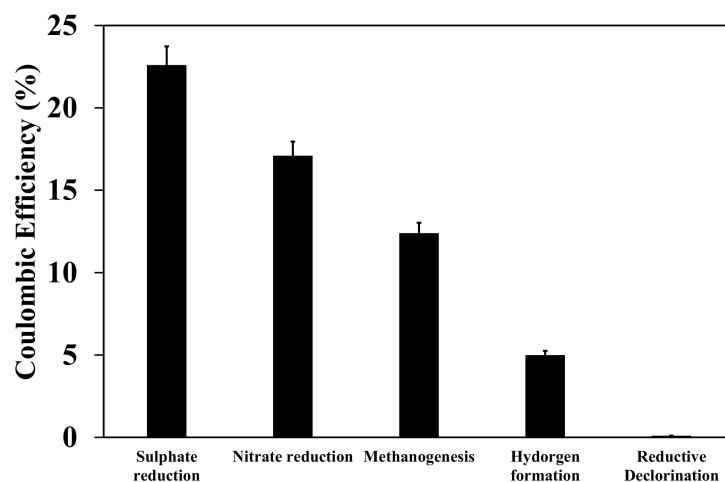

Figure 7. Coulombic efficiencies of the different reduction reactions at the sampling port D.

Table 2. Comparison of the data obtained in the present study with the previous internal counter-electrode configuration performances [35].

	PRB	Internal Counter-Electrode [35]
HRT (d^{-1})	0.8	1.2
RD (meq/Ld)	20 ± 11	134 ± 11
CE RD (%)	0.1 ± 0.1	2.1 ± 0.5
CE NO_3^- (%)	17 ± 2	12 ± 4
CE SO_4^{-2} (%)	22 ± 4	89 ± 7
Energy consumption (kWh/m^3)	4.6 ± 0.9	0.6 ± 0.1

3. Material and Methods

3.1. Bioelectrochemical Membrane-Less PBR-like Reactor

The bioelectrochemical scale-up reactor consisted of a borosilicate 1.05 m glass column with an internal diameter of 10 cm and an empty volume of 8.24 L (Figure 8). The same reactor geometry has been utilised for the realization of previous studies exploring the potential of the utilisation of the internal counter-electrode configuration [32]. The column was filled with conductive graphite granules with a diameter between 2 and 4 mm (Faima srl, Milano, Italy) and was held in place by two aluminium clamps to ensure air tightness. Differently from the lab scale reactor, there was no membrane, so the separation between cathodic/anodic zones was obtained by a thin layer (3 cm) of low conductivity material (silica beads). The electrical connections were ensured by placing graphite rod current collectors (with a diameter of 5 mm, Sigma-Aldrich, Milan, Italy) into each compartment. Ag/AgCl reference electrodes (+0.199 vs standard hydrogen electrode, SHE) (Amel, Milan, Italy) were placed in both chambers near the graphite rods to control the cathodic and the anodic potential. The cathode (working electrode), anode (counter electrode), and reference electrode were connected to a galvanostat-potentiostat Amel Model 551 (Milan,

Italy), which was used to set the cathodic current or the cathodic potential at the desired value. The PBR reactor was equipped with seven sampling ports, each with a threaded end (diameter 20 mm), positioned along the column and designated from A to G to characterize the system's performance. Port A served as the influent inlet, while port G served as the effluent outlet for up-flow mode operation. Sampling of the cathode was conducted through ports B and C, sampling of the low conductivity layer through port D, and sampling of the anode through ports E and F. (Figure 8).
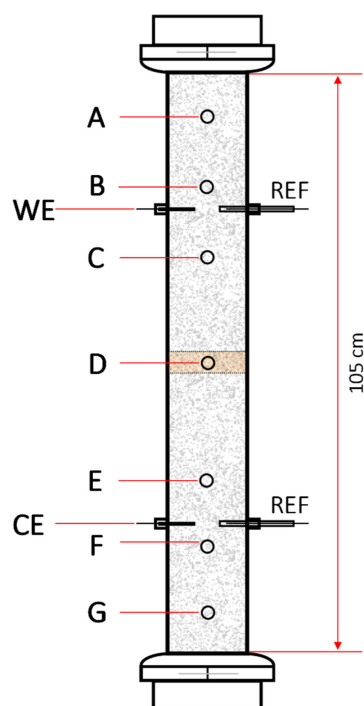

Figure 8. Bioelectrochemical membrane-less PBR-like reactor.

The influent was regulated by a peristaltic pump at a desired flow rate, and it was maintained in a self-collapsing Tedlar bag (25 L) (SKC Inc., Eighty Four, PA, USA) without headspace. The effluent was collected in a plastic tank equipped with an active carbon trap.

3.2. Bioelectrochemical Reactor Operating Conditions

Throughout the entire operational period, the reactor was operated in galvanostatic mode at 100 mA. The cathode chamber of the bioelectrochemical reactor was fed at a flow rate of 5.8 L/d. In the first operational period, the bioelectrochemical PBR reactor was fed with an anaerobic medium. The medium contained (g/L): NH_4Cl, 0.5; $MgCl_2$ $6H_2O$, 0.1; K_2HPO_4, 0.4; $MgCl_2$ 3 $2H_2O$, 0.05; 2 mL/L of a trace metal solution [39] and 2 mL/L of vitamin solution [40]. The electrical conductivity of the medium was 4.8 mS/cm, hence within the range of values typically reported for highly contaminated groundwater (i.e., 0.7 to 8.0 mS/cm). The pH of the medium was maintained between 7 and 7.5 with a buffer $NaHCO_3$ solution (10% *w/v*). Room temperature was maintained inside the reactor and in the sampling cells. The biotic test of the PBR reactor was conducted using a synthetic groundwater constituted by the same mineral medium composition with the addition of 35 mg/L nitrate, 150 mg/L sulphate and cisDCE to a final concentration of approximately 20 μmol/L. The reactor feed was supplied by using a self-collapsing Tedlar bag (25 L) without headspace. A tracer test to characterise the fluid-dynamic behaviour of the cathode compartment was carried out for each applied flow rate [17].

3.3. Analytical Procedures

Samples (5 mL), taken from each column reactor sampling port, were prepared in 10 mL glass vials and sealed with Teflon-faced butyl rubber stoppers and aluminium crimp caps. Previously, the vials were fluxed with N_2/CO_2 (70/30%). Headspace samples (100 μL) were taken from the reactors using gas-tight syringes and injected manually in a Varian 3400 (Varian, Palo Alto, CA, USA) gas-chromatograph equipped with a flame ionization detector (FID) for the quantification of volatile compounds (i.e., chloroethanes, chloroethenes, ethane, ethane, methane). The H_2 concentration was determined by gas chromatography with a thermal conductivity detector (TCD) (Varian 3400) or a reduction gas detector (RGD) (Trace Analytical TA3000R, Menlo Park, CA, USA) when the H_2 concentration was below a detectable limit. Calibration curves were then used to determine the nominal concentration in the liquid phase (i.e., assuming no partitioning of volatile compounds in the gas phase). Inorganic anions were determined by direct liquid injections (1 mL) of filtered (0.22 μm) liquid samples into an ionic chromatograph (Dionex ICS-1000 IC, Sunnyvale, CA, USA) equipped with a conductivity detector. The liquid phase was taken regularly (twice or three times a week), and Electric conductivity was measured by a conductometer to check the pH (WPA CM 35, Linton, Cambridge, UK). Total organic (TOC) and inorganic (IC) dissolved carbon were analysed with a TOC-CSV analyser (Shimadzu, Kyoto, Japan). All the chemicals used were of analytical grade and supplied by Sigma-Aldrich (Louis, MO, USA).

3.4. Data Elaboration

The rate and coulombic efficiency of TCE reductive dechlorination, methanogenesis, and anions reduction were calculated using established methods [17,34,35]. The calculation took into account the cathodic volume, which is the space from the top of the column to sampling port D. The rate of cis-DCE reduction in the continuous-flow reactor was determined by analysing the concentrations of its daughter products in the cathode effluent. Finally, the average rate was calculated as follows:

$$r_{RD}\left[\frac{\mu eq}{Ld}\right] = \frac{[VC]\cdot 2 + [ETH]\cdot 4 + [ETA]\cdot 6}{V_C}\cdot Q \tag{1}$$
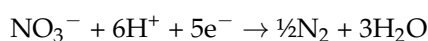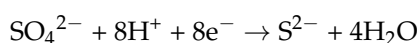
In the Equation, the concentrations (μM) of cis-DCE dechlorination products in the cathode effluent are represented by $[VC]$, $[ETH]$, and $[ETA]$. The number of moles of electrons required for their respective formation from 1 mol of cis-DCE are 2, 4, and 6. The flow rate is denoted as Q (L/d), while V_C represents the empty volume of the cathode chamber (L). The validity of this Equation is contingent on the condition that the feed contains only cis-DCE as the sole CAH, and no daughter products are present.

The reduction rates of sulphate and nitrate were averaged using the following similar method:

$$r_{sulfate}\left[\frac{\mu eq}{Ld}\right] = \frac{\Delta[sulfate]\cdot 8}{V_C}\cdot Q \tag{2}$$

$$r_{nitrate}\left[\frac{\mu eq}{Ld}\right] = \frac{\Delta[nitrate]\cdot 5}{V_C}\cdot Q \tag{3}$$

where $\Delta[sulphate]$ and $\Delta[nitrate]$ represent the concentration differences of the corresponding anions in the influent and effluent samples. The number of moles of electrons required for the reduction of 1 mol of each anion is 8 and 5, respectively. These values were determined based on the assumption of complete conversion through the following half-reactions [35]:

$$SO_4{}^{2-} + 8H^+ + 8e^- \rightarrow S^{2-} + 4H_2O$$

$$NO_3{}^- + 6H^+ + 5e^- \rightarrow \tfrac{1}{2}N_2 + 3H_2O$$

In a similar vein, the mean rate of methane generation was computed using the subsequent formula:

$$r_{CH_4}\left[\frac{\mu eq}{Ld}\right] = \frac{[CH_4]\cdot 8}{V_C}\cdot Q \tag{4}$$

here, $[CH_4]$ denotes the methane concentration in the effluent (μM), and 8 represents the number of electrons required to produce 1 mole of methane from the reduction of carbon dioxide.

The coulombic efficiency (ε%) for the RD of cis-DCE was calculated by comparing the theoretical electric current due to the formation of RD products to the actual electric current flowing through the system as follows:

$$\varepsilon_{RD}(\%) = \frac{\frac{r_{RD}\cdot V_C}{24\cdot 3600}\cdot F}{I}\cdot 100 \tag{5}$$

where F is the Faraday's constant (96,485 Cmol/electrons) and I is the electric current (μA). Likewise, the coulombic efficiencies for methanogenesis, sulphate reduction, and nitrate reduction were computed as follows:

$$\varepsilon_{CH_4}(\%) = \frac{\frac{r_{CH_4}\cdot V_C}{24\cdot 3600}\cdot F}{I}\cdot 100 \tag{6}$$

$$\varepsilon_{sulfate}(\%) = \frac{\frac{r_{sulfate}\cdot V_C}{24\cdot 3600}\cdot F}{I}\cdot 100 \tag{7}$$

$$\varepsilon_{nitrate}(\%) = \frac{\frac{r_{nitrate}\cdot V_C}{24\cdot 3600}\cdot F}{I}\cdot 100 \tag{8}$$

4. Conclusions

Scaling up of the system has been proven by a scale factor of ten (and likely appears to be feasible even at a higher scale factor) by using a column PBR-like reactor with downgradient groundwater flow and with no need for intermediate membrane separation. This latter makes it possible to simplify the required equipment and could significantly reduce the investment and operation costs. Using a synthetic medium, cisDCE removal with the formation of VC and non-chlorinated by-products was also proven in the membrane-less PBR reactor. Then, the presence of both the reductive dechlorination and anions reduction has also been verified by using synthetic groundwater in the presence of specialised dechlorinating electrophilic microorganisms. Those results open interesting perspectives towards further exploitation of the bioelectrochemical approach, in the view of remediation of contaminated groundwater for the removal of chlorinated solvents and of nitrate and sulphate as well. However, the low contact surface across the electrodes and a short electrode distance decreased the effective reactor portion available to enhance the biological reactions. In this configuration, the presence of a low-conductivity layer separating the two electrodes leads to a significant increase in the overvoltage effects, resulting in a notable rise in the potential difference within the cell compared to the previous studies. Hence, in this perspective, further studies will evaluate the increase of contact surface and the decrease of distance across the electrodes, together with an economic evaluation of cost reduction.

Author Contributions: G.S.: Writing—Original Draft, Writing-Review & Editing, L.L.: Writing—Original Draft, A.L.: Investigation Writing—Original Draft, M.P.P.: Supervision, M.Z.: Supervision, Writing—Original Draft, Writing-Review and Editing. All authors have read and agreed to the published version of the manuscript.

Data Availability Statement: Dataset available on request from the authors.

References

1. Bradley, P.M. History and Ecology of Chloroethene Biodegradation: A Review. *Bioremediation J.* **2003**, *7*, 81–109. [CrossRef]
2. Moran, M.J.; Zogorski, J.S.; Squillace, P.J. Chlorinated Solvents in Groundwater of the United States. *Environ. Sci. Technol.* **2007**, *41*, 74–81. [CrossRef] [PubMed]
3. McCarty, P.L. Groundwater Contamination by Chlorinated Solvents: History, Remediation Technologies and Strategies. In *In Situ Remediation of Chlorinated Solvent Plumes*; Stroo, H.F., Ward, C.H., Eds.; Springer: New York, NY, USA, 2010; pp. 1–28. [CrossRef]
4. Jugder, B.-E.; Ertan, H.; Bohl, S.; Lee, M.; Marquis, C.P.; Manefield, M. Organohalide Respiring Bacteria and Reductive Dehalogenases: Key Tools in Organohalide Bioremediation. *Front. Microbiol.* **2016**, *7*, 181210. [CrossRef] [PubMed]
5. Atashgahi, S.; Häggblom, M.M.; Smidt, H. Organohalide respiration in pristine environments: Implications for the natural halogen cycle. *Environ. Microbiol.* **2018**, *20*, 934–948. [CrossRef] [PubMed]
6. Atashgahi, S.; Lu, Y.; Smidt, H. Overview of Known Organohalide-Respiring Bacteria—Phylogenetic Diversity and Environmental Distribution. In *Organohalide-Respiring Bacteria*; Adrian, L., Löffler, F.E., Eds.; Springer: Berlin/Heidelberg, Germany, 2016; pp. 63–105. [CrossRef]
7. He, J.; Ritalahti, K.M.; Yang, K.-L.; Koenigsberg, S.S.; Löffler, F.E. Detoxification of vinyl chloride to ethene coupled to growth of an anaerobic bacterium. *Nature* **2003**, *424*, 62–65. [CrossRef] [PubMed]
8. Löffler, F.E.; Yan, J.; Ritalahti, K.M.; Adrian, L.; Edwards, E.A.; Konstantinidis, K.T.; Müller, J.A.; Fullerton, H.; Zinder, S.H.; Spormann, A.M. *Dehalococcoides mccartyi* gen. nov., sp. nov., obligately organohalide-respiring anaerobic bacteria relevant to halogen cycling and bioremediation, belong to a novel bacterial class, *Dehalococcoidia* classis nov., order *Dehalococcoidales* ord. nov. and family *Dehalococcoidaceae* fam. nov., within the phylum *Chloroflexi*. *Int. J. Syst. Evol. Microbiol.* **2013**, *63 Pt 2*, 625–635. [CrossRef] [PubMed]
9. Lohner, S.T.; Deutzmann, J.S.; Logan, B.E.; Leigh, J.; Spormann, A.M. Hydrogenase-independent uptake and metabolism of electrons by the archaeon *Methanococcus maripaludis*. *ISME J.* **2014**, *8*, 1673–1681. [CrossRef]
10. Roubaud, E.; Lacroix, R.; Da Silva, S.; Bergel, A.; Basséguy, R.; Erable, B. Catalysis of the hydrogen evolution reaction by hydrogen carbonate to decrease the voltage of microbial electrolysis cell fed with domestic wastewater. *Electrochim. Acta* **2018**, *275*, 32–39. [CrossRef]
11. Lacroix, R.; Roubaud, E.; Erable, B.; Etcheverry, L.; Bergel, A.; Basséguy, R.; Da Silva, S. Design of 3D microbial anodes for microbial electrolysis cells (MEC) fuelled by domestic wastewater. Part I: Multiphysics modelling. *J. Environ. Chem. Eng.* **2021**, *9*, 105476. [CrossRef]
12. Cristiani, L.; Zeppilli, M.; Porcu, C.; Majone, M. Ammonium Recovery and Biogas Upgrading in a Tubular Micro-Pilot Microbial Electrolysis Cell (MEC). *Molecules* **2020**, *25*, 2723. [CrossRef]
13. Ceballos-Escalera, A.; Pous, N.; Balaguer, M.D.; Puig, S. Electrochemical water softening as pretreatment for nitrate electro bioremediation. *Sci. Total Environ.* **2022**, *806*, 150433. [CrossRef]
14. Wang, X.; Aulenta, F.; Puig, S.; Esteve-Núñez, A.; He, Y.; Mu, Y.; Rabaey, K. Microbial electrochemistry for bioremediation. *Environ. Sci. Ecotechnol.* **2020**, *1*, 100013. [CrossRef] [PubMed]
15. Rosenbaum, M.; Aulenta, F.; Villano, M.; Angenent, L.T. Cathodes as electron donors for microbial metabolism: Which extracellular electron transfer mechanisms are involved? *Bioresour. Technol.* **2011**, *102*, 324–333. [CrossRef] [PubMed]
16. Majone, M.; Verdini, R.; Aulenta, F.; Rossetti, S.; Tandoi, V.; Kalogerakis, N.; Agathos, S.; Puig, S.; Zanaroli, G.; Fava, F. In situ groundwater and sediment bioremediation: Barriers and perspectives at European contaminated sites. *New Biotechnol.* **2015**, *32*, 133–146. [CrossRef]
17. Verdini, R.; Aulenta, F.; de Tora, F.; Lai, A.; Majone, M. Relative contribution of set cathode potential and external mass transport on TCE dechlorination in a continuous-flow bioelectrochemical reactor. *Chemosphere* **2015**, *136*, 72–78. [CrossRef] [PubMed]
18. Xiao, Z.; Jiang, W.; Chen, D.; Xu, Y. Bioremediation of typical chlorinated hydrocarbons by microbial reductive dechlorination and its key players: A review. *Ecotoxicol. Environ. Saf.* **2020**, *202*, 110925. [CrossRef] [PubMed]
19. Aulenta, F.; Maio, V.D.; Ferri, T.; Majone, M. The humic acid analogue antraquinone-2,6-disulfonate (AQDS) serves as an electron shuttle in the electricity-driven microbial dechlorination of trichloroethene to cis-dichloroethene. *Bioresour. Technol.* **2010**, *101*, 9728–9733. [CrossRef]
20. Rabaey, K.; Angenent, L.; Schröder, U.; Keller, J. Bioelectrochemical systems: From extracellular electron transfer to biotechnological application. *Water Intell. Online* **2009**, *8*, 9781780401621. [CrossRef]
21. Tiehm, A.; Schmidt, K.R. Sequential anaerobic/aerobic biodegradation of chloroethenes—Aspects of field application. *Curr. Opin. Biotechnol.* **2011**, *22*, 415–421. [CrossRef] [PubMed]
22. Mattes, T.E.; Alexander, A.K.; Coleman, N.V. Aerobic biodegradation of the chloroethenes: Pathways, enzymes, ecology, and evolution. *FEMS Microbiol. Rev.* **2010**, *34*, 445–475. [CrossRef]

23. Mattes, T.E.; Jin, Y.O.; Livermore, J.; Pearl, M.; Liu, X. Abundance and activity of vinyl chloride (VC)-oxidizing bacteria in a dilute groundwater VC plume biostimulated with oxygen and ethene. *Appl. Microbiol. Biotechnol.* **2015**, *99*, 9267–9276. [CrossRef] [PubMed]

24. Lohner, S.T.; Becker, D.; Mangold, K.-M.; Tiehm, A. Sequential Reductive and Oxidative Biodegradation of Chloroethenes Stimulated in a Coupled Bioelectro-Process. *Environ. Sci. Technol.* **2011**, *45*, 6491–6497. [CrossRef]

25. Pant, P.; Pant, S. A review: Advances in microbial remediation of trichloroethylene (TCE). *J. Environ. Sci.* **2010**, *22*, 116–126. [CrossRef] [PubMed]

26. Liu, X.; Shi, L.; Gu, J.-D. Microbial electrocatalysis: Redox mediators responsible for extracellular electron transfer. *Biotechnol. Adv.* **2018**, *36*, 1815–1827. [CrossRef] [PubMed]

27. Lovley, D.R. Extracellular electron transfer: Wires, capacitors, iron lungs, and more. *Geobiology* **2008**, *6*, 225–231. [CrossRef]

28. Vogel, M.; Kopinke, F.-D.; Mackenzie, K. Acceleration of microiron-based dechlorination in water by contact with fibrous activated carbon. *Sci. Total Environ.* **2019**, *660*, 1274–1282. [CrossRef] [PubMed]

29. Hoareau, M.; Etcheverry, L.; Chapleur, O.; Bureau, C.; Midoux, C.; Erable, B.; Bergel, A. The electrochemical microbial tree: A new concept for wastewater treatment. *Chem. Eng. J.* **2023**, *454*, 140295. [CrossRef]

30. Gonzalez-Nava, C.; Manríquez, J.; Godínez, L.A.; Rodríguez-Valadez, F.J. Enhancement of the electron transfer and ion transport phenomena in microbial fuel cells containing humic acid-modified bioanodes. *Bioelectrochemistry* **2022**, *144*, 108003. [CrossRef]

31. Aulenta, F.; Catervi, A.; Majone, M.; Panero, S.; Reale, P.; Rossetti, S. Electron Transfer from a Solid-State Electrode Assisted by Methyl Viologen Sustains Efficient Microbial Reductive Dechlorination of TCE. *Environ. Sci. Technol.* **2007**, *41*, 2554–2559. [CrossRef]

32. Lai, A.; Verdini, R.; Aulenta, F.; Majone, M. Influence of nitrate and sulfate reduction in the bioelectrochemically assisted dechlorination of cis-DCE. *Chemosphere* **2015**, *125*, 147–154. [CrossRef]

33. Zeppilli, M.; Dell'Armi, E.; Cristiani, L.; Papini, M.P.; Majone, M. Reductive/Oxidative Sequential Bioelectrochemical Process for Perchloroethylene Removal. *Water* **2019**, *11*, 2579. [CrossRef]

34. Tucci, M.; Fernández-Verdejo, D.; Resitano, M.; Ciacia, P.; Guisasola, A.; Blánquez, P.; Marco-Urrea, E.; Viggi, C.C.; Matturro, B.; Crognale, S.; et al. Toluene-driven anaerobic biodegradation of chloroform in a continuous-flow bioelectrochemical reactor. *Chemosphere* **2023**, *338*, 139467. [CrossRef] [PubMed]

35. Dell'Armi, E.; Zeppilli, M.; De Santis, F.; Papini, M.P.; Majone, M. Control of Sulfate and Nitrate Reduction by Setting Hydraulic Retention Time and Applied Potential on a Membraneless Microbial Electrolysis Cell for Perchloroethylene Removal. *ACS Omega* **2021**, *6*, 25211–25218. [CrossRef] [PubMed]

36. Dell'Armi, E.; Zeppilli, M.; Di Franca, M.L.; Matturro, B.; Feigl, V.; Molnár, M.; Berkl, Z.; Németh, I.; Yaqoubi, H.; Rossetti, S.; et al. Evaluation of a bioelectrochemical reductive/oxidative sequential process for chlorinated aliphatic hydrocarbons (CAHs) removal from a real contaminated groundwater. *J. Water Process Eng.* **2022**, *49*, 103101. [CrossRef]

37. Field, J.A.; Sierra-Alvarez, R. Biodegradability of chlorinated solvents and related chlorinated aliphatic compounds. *Rev. Environ. Sci. Biotechnol.* **2004**, *3*, 185–254. [CrossRef]

38. Lin, H.-W.; Kustermans, C.; Vaiopoulou, E.; Prévoteau, A.; Rabaey, K.; Yuan, Z.; Pikaar, I. Electrochemical oxidation of iron and alkalinity generation for efficient sulfide control in sewers. *Water Res.* **2017**, *118*, 114–120. [CrossRef]

39. Zeikus, J.G. The biology of methanogenic bacteria. *Bacteriol. Rev.* **1977**, *41*, 514–541. [CrossRef]

40. Balch, W.E.; Fox, G.E.; Magrum, L.J.; Woese, C.R.; Wolfe, R.S. Methanogens: Reevaluation of a unique biological group. *Microbiol. Rev.* **1979**, *43*, 260–296. [CrossRef]